# Direct Extracellular Interaction between Carbonic Anhydrase IV and the Human NBC1 Sodium/Bicarbonate Co-Transporter†

Bernardo V. Alvarez,‡ Frederick B. Loiselle,‡ Claudiu T. Supuran,§ George J. Schwartz,|| and Joseph R. Casey*,‡

*Department of Physiology and Department of Biochemistry, University of Alberta, Edmonton, Alberta, Canada T6G 2H7, University of Florence, Dipartimento di Chimica Laboratorio di Chimica Bioinorganica, Sesto Fiorentino, Italy, and Department of Pediatrics, University of Rochester, Rochester, New York 14642-8408*

*Received July 24, 2003; Revised Manuscript Received August 27, 2003*

ABSTRACT: Sodium/bicarbonate co-transporters (NBC) are crucial in the regulation of intracellular pH ($pH_i$) and $HCO_3^-$ metabolism. Electrogenic NBC1 catalyzes $HCO_3^-$ fluxes in mammalian kidney, pancreas, and heart cells. Carbonic anhydrase IV (CAIV), which is also present in these tissues, is glycosylphosphatidyl inositol-anchored to the outer surface of the plasma membrane where it catalyzes the hydration−dehydration of $CO_2/HCO_3^-$. The physical and functional interactions of CAIV and NBC1 were investigated. NBC1 activity was measured by changes of $pH_i$ in NBC1-transfected HEK293 cells subjected to acid loads. Cotransfection of CAIV with NBC1 increased the rate of $pH_i$ recovery by 44 ± 3%, as compared to NBC1-alone. In contrast, CAIV did not increase the functional activity of G767T-NBC1 (mutated on the fourth extracellular loop (EC4) of NBC1), and G767T-NBC1, unlike wild-type NBC1, did not interact with CAIV in glutathione-*S*-transferase pull-down assays. This indicates that G767 of NBC1 is directly involved in CAIV interaction. NBC1-mediated $pH_i$ recovery rate after acid load was inhibited by 40 ± 7% when coexpressed with the inactive human CAII mutant, V143Y. V143Y CAII competes with endogenous CAII for interaction with NBC1 at the inner surface of the plasma membrane, which indicates that NBC1/CAII interaction is needed for full $pH_i$ recovery activity. We conclude that CAIV binds EC4 of NBC1, and this interaction is essential for full NBC1 activity. The tethering of CAII and CAIV close to the NBC1 $HCO_3^-$ transport site maximizes the transmembrane $HCO_3^-$ gradient local to NBC1 and thereby activates the transport rate.

The electrogenic sodium/bicarbonate co-transporter (NBC1) mediates $Na^+$-coupled $HCO_3^-$ transport across plasma membranes of many mammalian cells (*1*) to regulate $HCO_3^-$ secretion/absorption, $HCO_3^-$ metabolism, and intracellular pH ($pH_i$) (*2*). NBC1, the first mammalian NBC sequence reported, was cloned from human kidney (*3*). NBC1a (also called kNBC1) has an essential role in $HCO_3^-$ reabsorption in basolateral membranes (BLM) of the proximal tubule, where it works in tandem with luminal $H^+$ transporters (NHE3 and $H^+$-ATPase) to secrete acid (*4*). With an apparent stoichiometry of $3HCO_3^-$ per $Na^+$ (*5*), NBC1a mediates $HCO_3^-$ efflux from the cell to the blood, resulting in a cellular acidification (*6*, *7*).

The NBC1b splicing variant (also called pNBC1 or hhNBC), found in pancreas and heart (*8*, *9*), is identical to NBC1a over the C-terminal 994 amino acids, including the entire membrane domain. NBC1b has a unique N-terminus of 85 amino acids that replaces the initial 41 amino acids of NBC1a. NBC1b in BLM of pancreatic duct cells has a stoichiometry of $2HCO_3^-$:$1Na^+$ and transports $HCO_3^-$ into the cell (*10*). NBC1b is important for the secretion of $HCO_3^-$-rich fluid from the pancreas and also mediates $HCO_3^-$ uptake in isolated rat cardiomyocytes, defending cells against acid loading (*11*).

The 14 mammalian carbonic anhydrases (CA)[1] designated I-XIV (*12*) are functionally linked to NBCs because CAs catalyze the reversible hydration of carbon dioxide ($CO_2 + H_2O \leftrightarrow HCO_3^- + H^+$), thus producing and consuming the substrate for transport by NBC1. Cytosolic isozyme CAII and membrane-associated CAIV are key to renal $HCO_3^-$ reabsorption (*12*). CAIV is posttranslationally cleaved and modified with a C-terminal glycosylphosphatidyl inositol (GPI) tail, which anchors the protein to the extracellular surface. The identification of CAIV in proximal tubule BLM (*13*) suggests a role of this isozyme in renal $HCO_3^-$ transport

† Supported by an operating grant from the Canadian Institutes of Health Research (J.R.C.) and USPHS DK-50603 (G.J.S.). B.V.A. holds a postdoctoral fellowship from the Alberta Heritage Foundation for Medical Research (AHFMR). F.B.L. is supported by a Natural Sciences and Engineering Research Council (Canada) studentship. J.R.C. is a Senior Scholar of AHFMR.

* Corresponding author. Phone: (780) 492-7203. Fax: (780) 492-8915. E-mail: joe.casey@ualberta.ca.

‡ University of Alberta.

§ University of Florence.

|| University of Rochester.

[1] Abreviations: ACTZ, acetazolamide; AE, $Cl^-/HCO_3^-$ anion exchanger; BCECF-AM, 2′,7′-bis(2-carboxyethyl)-5(6)-carboxyfluorescein-acetoxymethyl ester; CA, carbonic anhydrase; DRA, downregulated in adenoma; EC, extracellular loop; ECL, enhanced chemiluminescence; GPI, glycosylphosphatidyl inositol; GST, glutathione-*S*-transferase; GST-NBC1EC3, fusion of the third extracellular loop of NBC1 to GST; GST-NBC1EC4, fusion of the fourth extracellular loop of NBC1 to GST; HEK, human embryonic kidney; NBC, sodium/bicarbonate co-transporter; $pH_i$, intracellular pH; PMSF, phenylmethylsulfonyl fluoride; SDS, sodium dodecyl sulfate; SDS−PAGE, SDS−polyacrylamide gel electrophoresis; TLCK, *N*-*p*-tosyl-L-lysine chloromethyl ketone; TPCK, *N*-tosyl-L-phenylalanine.

10.1021/bi0353124 CCC: $25.00 
Published on Web 10/01/2003

and colocalizes NBC1 and CAIV. The pancreas also expresses CAIV, which may form a mutually complementary system with CAII to regulate the luminal pH of the human pancreatic duct system (*14*). No cytosolic CA was detectable in cardiac muscle, but CAIV is present in the heart (*15*). A significant role for CAIV in cardiac pH regulation has been suggested (*16*).

Interactions between AE $Cl^-/HCO_3^-$ exchangers and both cytosolic CAII and extracellular CAIV have been identified as essential for full bicarbonate transport activity (*17*−*19*). In the present study, we have identified functional and physical interactions between human NBC1b and both CAII and CAIV. The expression of functionally inactive CAII inhibited transport activity of NBC1 due to the displacement of endogenous wild-type CAII from a cytoplasmic binding site, as observed for AE1. The observation of physical and functional interactions between CAII and NBC1 confirms a recent report (*20*). Here, GST pull-down and gel overlay assays revealed that there is a physical interaction between extracellular CAIV and the NBC1 co-transporter that occurs via the fourth extracellular loop (EC) of NBC1. Expression of CAIV increased the activity of NBC1b. However, the mutation of EC4 of NBC1 blocked the physical and functional interactions between CAIV and NBC1. Although the EC4 mutant of NBC1b was functionally active, the mutant's transport activity did not rise in the presence of CAIV.

In light of our previous findings with AE1, we now suggest that the interaction of bicarbonate transporters with intracellular and extracellular carbonic anhydrases is a universal component of bicarbonate transport physiology. Furthermore, this work suggests a general mechanism to modulate membrane transport activity: the interaction between peripheral enzymes and membrane transport proteins that move the product of the enzyme.

## MATERIALS AND METHODS

*Molecular Biology*. Expression constructs for rabbit CAIV (*21*), human NBC1b (*9*), and CAII (*18*) have been described previously. The NBC1 G767T mutant was constructed by megaprimer mutagenesis (*22*). Bacterial expression constructs encoding GST fusion proteins consisting of the cDNA for GST fused to either cDNA corresponding to the third (amino acids 603−689) or fourth (amino acids 748−779) extracellular loop (EC) of NBC1b and fourth loop of rat AE3 (amino acids 944−975) were constructed. In each case, cDNA sequences were amplified by PCR, and primers contained Bam HI restriction sites at their 5′ and 3′ ends to facilitate cloning of the PCR product into the Bam HI site of pGEX-5X-3 (Pharmacia Biotech).

*Protein Expression and GST Pull-Down Assays*. NBC and CA proteins were expressed by transient transfection of the human kidney origin cell line, HEK293 (*11*, *18*), using the calcium phosphate method (*23*). Cells were grown at 37 °C in an air/$CO_2$ (19:1) environment in DMEM medium, supplemented with 5% (v/v) fetal bovine serum and 5% (v/v) calf serum. GST fusion proteins were expressed and purified as previously described (*19*). In GST pull-down assays, 250 $\mu$g of GST, GST-NBC1EC3, or GST-NBC1EC4 was bound to 40 $\mu$L of glutathione sepharose resin. Cell lysates of CAIV-transfected cells were prepared by solubilization in 150 $\mu$L of IPB buffer ((1% (v/v) NP40, 5 mM EDTA, 150 mM NaCl, 0.5% (w/v) sodium deoxycholate, 10 mM Tris-HCl, pH 7.50)), supplemented with protease inhibitors (Complete Mini, protease inhibitor, Roche). Lysates were applied to the resin and eluted (*19*).

*Immunoprecipitation.* Membrane protein from mouse kidney (1.35 mg) was incubated with appropriate antibody for 4 h at 4 °C and then with washed protein A/G beads (Ultralink, Pierce) overnight. The resin was washed and then boiled in SDS−PAGE sample buffer. Solubilized complexes, along with separate aliquots of mouse kidney membranes (100 $\mu$g), were fractionated by SDS−PAGE and transferred to nitrocellulose.

*Immunodetection.* HEK293 cells were transfected or cotransfected with NBC1b, CAIV, CAII, and mutant V143Y CAII cDNAs (*9*). Two days post-transfection, cells were washed in PBS buffer, and lysates of the whole tissue culture cells were prepared by the addition of 150 $\mu$L of SDS−PAGE sample buffer. Samples (5 $\mu$g of protein) were resolved by SDS−PAGE on 12% acrylamide gels (*24*). Proteins were transferred to PVDF membranes and then incubated with either rabbit anti-rat NBC1 antibody, sheep anti-human CAII antibody (Serotec), goat anti-mouse CAIV antibody (Santa Cruz Biotechnology), or goat anti-rabbit CAIV (*19*). To normalize for the amount of GST, or GST fusion protein, membranes used for GST pull-down assays were stripped by 10 min incubation with stripping buffer (100 mM 2-mercaptoethanol, 62.5 mM Tris-HCl, pH 6.8) at 50 °C. Membranes were blocked with 5% nonfat milk and reprobed with anti-GST (Z-5) rabbit polyclonal antibody (Santa Cruz Biotechnology). Immunoblots were incubated with either donkey anti-rabbit IgG conjugated to horseradish peroxidase, or donkey anti-sheep IgG conjugated to horseradish peroxidase, or rabbit anti-goat IgG conjugated to horseradish peroxidase (*19*). Blots were visualized and quantified using the ECL reagent and a Kodak Image Station.

*Gel Overlay Assays.* Gel overlay assays to detect NBC1 interactions with CAII and CAIV were performed as previously described (*18*, *19*). Briefly, HEK293 cells grown in 60 mm culture dishes were transiently transfected individually with cDNA encoding NBC1b or CAIV, as described previously. Two days post-transfection, cells expressing an NBC1b protein were solubilized in SDS−PAGE sample buffer, and cells expressing CAIV were solubilized in 200 $\mu$L of IPB buffer supplemented with protease inhibitors. Samples were sheared and centrifuged as described previously. Immunoblots of lysates of cells transfected with NBC1b cDNA were prepared as described previously. Immunoblots were blocked for 2 h with 10% TBST-M and then incubated overnight in 5% TBST-M containing 200 $\mu$L of the cell lysate prepared from CAIV transfected cells. Immunoblots were then washed 3 × 10 min in TBST and then probed for CAIV as previously described.

*Assay of NBC1b Activity.* NBC1b activity was monitored using a fluorescence assay (*11*). Briefly, HEK293 cells grown on poly-L-lysine coated coverslips were transiently transfected. Two days post-transfection, coverslips were rinsed in serum free DMEM and incubated in 4 mL of serum-free media, containing 2 $\mu$M BCECF-AM (37 °C, 20 min). Coverslips were mounted in a cuvette and perfused with bicarbonate buffer (128.3 mM NaCl, 4.5 mM KCl, 1.35 mM $CaCl_2$, 20.23 mM $NaHCO_3$, 1.05 $MgSO_4$, 11 mM glucose,

pH 7.40) equilibrated with 5% $CO_2$/air. $HCO_3^-$ transport activity of NBC1b ($J_{HCO_3^-}$) was measured during the recovery from transient intracellular acidification. Cells were acid loaded by perfusion with bicarbonate buffer, containing 20 mM $NH_4Cl$ for 4−5 min, followed by the wash-out of $NH_4Cl$ with bicarbonate buffer. Assays were performed in the presence of 5 $\mu$M EIPA ((5-(*N*-ethyl-*N*-isopropyl) amiloride (Sigma)) to block $Na^+/H^+$ exchanger (NHE) activity. The fluorescence was monitored in a Photon Technologies International RCR fluorimeter, at excitation wavelengths of 440 and 500 nm and an emission of 530 nm. Fluorescence ratios were converted to $pH_i$ by the nigericin/high potassium technique at three pH values between 6.5 and 7.5 (*25*). The initial rate of $pH_i$ recovery from an acid load was calculated by fitting a linear regression of either the first 1 or 3 min of the $pH_i$ recovery after maximum acidosis. Rates of $HCO_3^-$ influx ($J_{HCO_3^-}$in mM/min) were estimated as described previously (*19*). In all cases, the transport activity of sham-transfected cells was subtracted from the total rate to ensure that these rates consisted only of NBC1b transport activity.

*Statistical Analysis.* Statistical significance was evaluated using an unpaired *t*-test and one-way ANOVA, with $p < 0.05$ considered significant. Error bars show standard error of the mean ($n = 3-5$).

## RESULTS

*NBC1b Activity in HEK293 Cells.* HEK293 cells, transfected with human NBC1b cDNA and loaded with BCECF-AM fluorescent dye to measure $pH_i$, were perfused with bicarbonate buffer and subjected to $NH_4Cl$ pre-pulses. Figure 1A shows robust $pH_i$ recovery following acid load due to the NBC1b activity. The transport rate for HEK293 cells transfected with NBC1b cDNA was 2.55 ± 0.30 mM/min ($n = 4$) after the correction for the background recovery rate of sham transfected cells (0.53 ± 0.05 mM/min, $n = 4$). $pH_i$ recovery activity in NBC1-transfected cells was 96 ± 0.2% ($n = 3$; $p < 0.05$) inhibited by 1 mM DIDS, consistent with NBC1 (Figures 1A and 2).

Gel overlay assays showed that CAII interacted specifically with NBC1b (data not shown), which confirms a recent observation (*20*). To examine the functional role of the CAII/NBC1b interaction, we performed a dominant negative experiment, where the functionally inactive CAII mutant, V143Y, expressed in HEK293 cells at approximately 20-fold over the endogenous CAII level (*18*), can displace wild-type CAII from cellular binding sites. NBC1b-transfected HEK293 cells were cotransfected with cDNA for V143Y CAII. The rate of NBC1b-mediated recovery of $pH_i$ after acid load was reduced by 61%, to 0.99 ± 0.03 mM/min ($n = 4$, $p < 0.05$), in the presence of V143Y CAII mutant (Figures 1B, 2). Overexpression of wild-type human CAII did not affect the transport activity of NBC1b (2.49 ± 0.40 mM/min, $n = 3$) (data not shown). We conclude that the binding of cytoplasmic CAII to NBC1b increases the rate at which NBC1b alkalinizes the cell.

*Functional Interaction between CAIV and NBC1b.* The functional interaction between CAIV and NBC1b was studied in HEK293 cells, which do not endogenously express CAIV, as assessed on immunoblots and by the failure of membrane impermeant carbonic anhydrase inhibitor to inhibit CA activity in untransfected HEK293 cells (*26*). Cotransfection

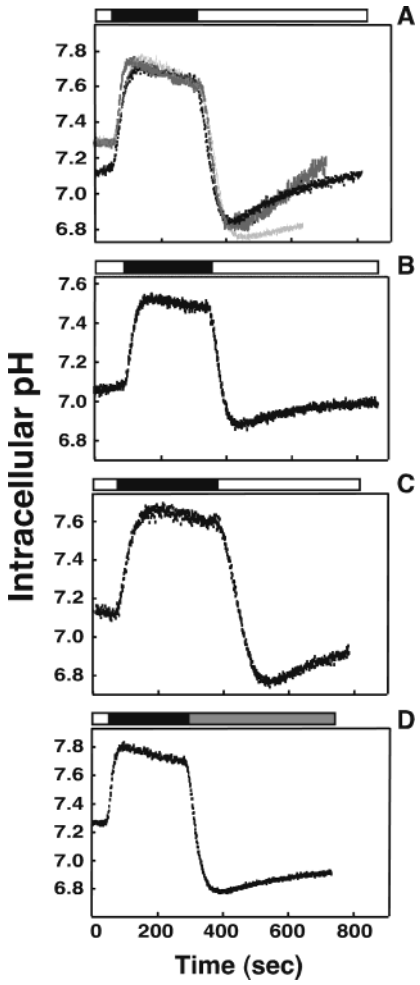


FIGURE 1: Effect of carbonic anhydrase II and IV on NBC1b transport activity. HEK293 cells were transiently cotransfected with cDNAs. (A) NBC1b (black), NBC1b incubated with 1 mM DIDS (light gray), and NBC1b/CAIV (dark gray). (B) NBC1b and V143Y CAII. (C and D) NBC1b, V143Y CAII, and CAIV. Cells were loaded with BCECF-AM and placed into a fluorimeter to monitor $pH_i$. Cells were perfused alternately with bicarbonate buffer (open bar), bicarbonate buffer containing 20 mM $NH_4Cl$ (black bar), or bicarbonate buffer containing 200 $\mu$M acetazolamide (gray bar).

of HEK293 cells with CAIV and NBC1b increased transport activity by 44 ± 3% relative to NBC1b alone (Figures 1A and 2). HEK293 cells were also cotransfected with NBC1, V143Y CAII, and CAIV, and transport assays were performed. Figures 1C and 2 show that the impaired $pH_i$ recovery due to the V143Y CAII was rescued by CAIV expression. Transport rates were not different from cells transfected with NBC1b alone (2.35 ± 0.20 mM/min, $n = 4$). To examine the role of CAIV in the process, transport was measured in the presence of the CA inhibitor, acetazolamide (Figure 1D). Acetazolamide (ACTZ) abolished the CAIV-induced rescue of NBC1b transport activity (0.80 ± 0.10 mM/min, $n = 3$, $p < 0.05$). Similarly, in NBC1b/V143Y CAII/CAIV cotransfected cells, the membrane-impermeant carbonic anhydrase inhibitor, 1-[5-sulfamoyl-1,3,4-thiadiazol-2-yl-(aminosulfonyl-4-phenyl)]-2,6 dimethyl-4-phenyl-pyridinium perchlorate (40 nM) (*27*), reduced NBC1b activity by 70 ± 3% ($n = 3$) (data not shown), which indicates that CAIV on the cell surface is responsible for the rescue of NBC1b activity.

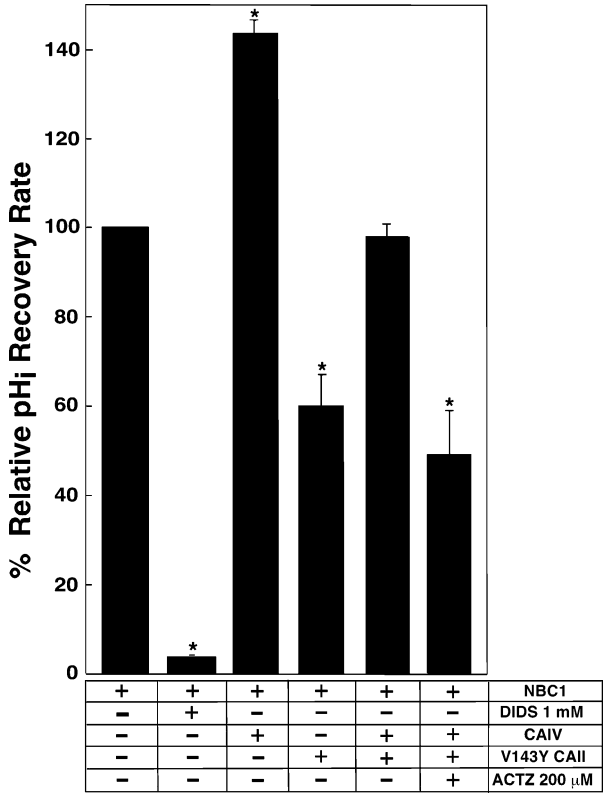


FIGURE 2: Summary of NBC1 transport activity. Mean transport rates, expressed relative to rate for HEK293 cells transfected with NBC1 alone. Asterisk represents statistical significance.

Figure 2 summarizes NBC1b transport activity under different conditions of CA activity. The initial fall in $pH_i$ was similar in all six groups, reaching an acid load peak of pH 6.96 ± 0.10 (NBC1b), 6.74 ± 0.01 (NBC1b + DIDS), 6.77 ± 0.04 (NBC1b/CAIV), 6.98 ± 0.05 (NBC1b/V143Y CAII), 6.84 ± 0.10 (NBC1b/V143Y CAII/CAIV) ($n = 4$), and 6.80 ± 0.10 (NBC1b/V143Y CAII/CAIV + ACTZ) ($n = 3$), respectively, for the four samples (not significant, one-way ANOVA). Figure 2 shows that the transport activity of NBC1b-transfected HEK293 cells, which is maximally inhibited by 40 ± 7% ($n = 4$, $p < 0.05$) by V143Y CAII expression, can be completely rescued by the expression of CAIV (98 ± 3%, $n = 4$).

Gel overlay assays (Figure 3), with NBC1b on the blot overlaid with CAIV-containing lysates, showed that CAIV bound NBC1b, but this interaction was not reduced by 200 μM acetazolamide ($1.8 \pm 0.2 \times 10^4$ pixels of CAIV without acetazolamide and $1.9 \pm 0.1 \times 10^4$ pixels with acetazolamide). This confirms that the effect of acetazolamide is mediated through its inhibition of CAIV catalytic activity, not the disruption of the NBC1b/CAIV interaction. On the basis of these results, we propose that CAIV functionally interacts with NBC1b, forming an extracellular membrane protein complex involved in the regulation of bicarbonate metabolism and $pH_i$.

In a human pancreatic duct cell line, the processing of CAIV to the cell surface is dependent on the expression of the CFTR $Cl^-$ channel (*28*). To examine the effect of CAIV on NBC1b cell surface processing, we expressed NBC1b either alone or along with CAIV in cotransfected HEK293 cells and monitored cell surface processing with a cell surface biotinylation assay (*29*). Assays revealed that CAIV did not affect the efficiency of NBC1b cell surface expression (28 ± 3% for NBC1b alone and 28 ± 9% for NBC1b/CAIV) (not shown).

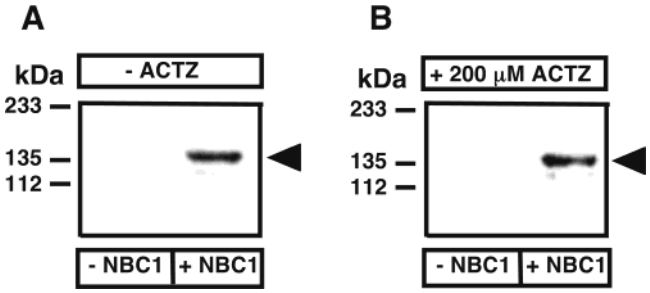


FIGURE 3: Blot overlay assay of CAIV on NBC1b. HEK293 cells were transiently transfected individually with vector alone (−NBC1) or with NBC1b (+NBC1) cDNA. Two days post-transfection, cells were solubilized, and 5 μg of protein was resolved by SDS−PAGE on 7.5% acrylamide gels and transferred to a PVDF membrane, as indicated. Immunoblots were blocked for 2 h with 10% TST-M and then incubated overnight in 5% TBST-M containing a lysate of CAIV-transfected HEK293 cells. (A) CAIV lysates in the absence of 200 μM acetazolamide (ACTZ). (B) CAIV lysates in the presence 200 μM ACTZ. Arrows indicate the position of the NBC1b.

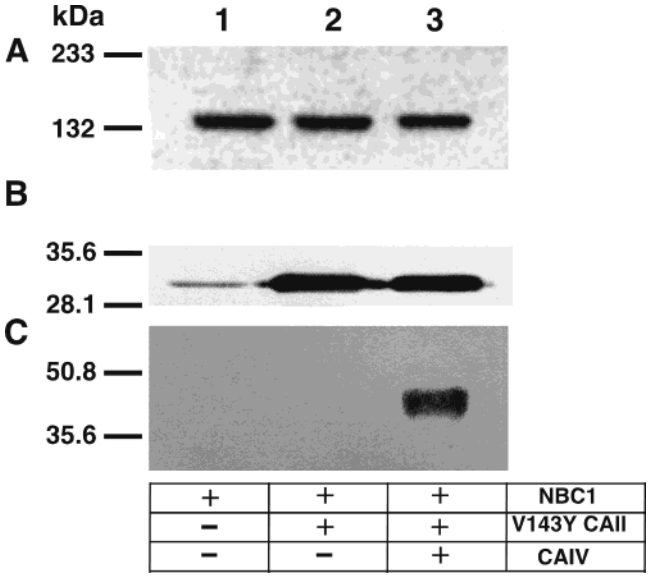


FIGURE 4: Expression of NBC1, CAII, and CAIV. HEK293 cells were transiently cotransfected with cDNA coding for NBC1b, CAII V143Y, and CAIV, as indicated. Two days post-transfection, cells were solubilized, and samples (5 μg of protein) were analyzed on immunoblots probed with (A) rabbit polyclonal anti-rat NBC1 antibody, (B) sheep-anti human CAII antibody, or (C) goat anti-rabbit CAIV antibody.

*Expression of NBC1b and CA in HEK293 Cells.* Differences in NBC1b activity could result from differential levels of protein expression. To assess this possibility, HEK293 cells were transiently cotransfected with cDNAs encoding NBC1b, the functionally inactive mutant CAII V143Y, and CAIV. Figure 4A−C shows that HEK293 cells expressed similar levels of NBC1b, whether expressed alone or coexpressed with V143Y CAII and/or CAIV. Thus, the changes of NBC1b activity observed upon coexpression of V143Y CAII and CAIV did not result from changes of the NBC1b expression. Cells transfected with vector alone showed no immunoreactivity with NBC1b or CAIV antibodies (not shown), but transfection clearly resulted in the

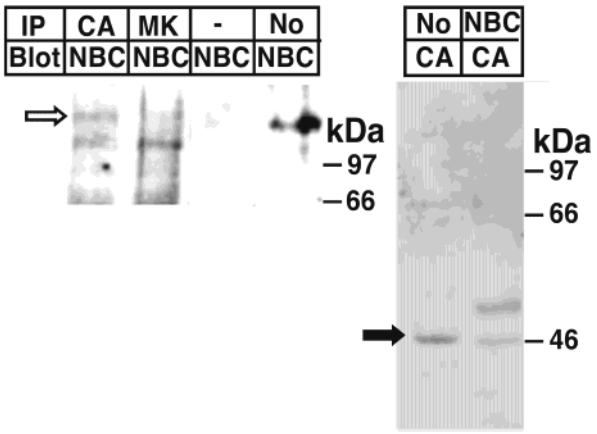


FIGURE 5: Immunoprecipitation of NBC1/CAIV complex from kidney. Lysate (1.35 mg of protein for immunoprecipitates and 100 $\mu$g of protein for nonprecipitated samples) from kidney membranes was immunoprecipitated (IP) with antibody directed against NBC1 (NBC), CAIV (CA), irrelevant phospho-p44/42 MAP kinase (MK), without antibody (−), or was directly loaded onto the gel with no immunoprecipitation (No). Samples were electrophoresed on 10% acrylamide gels, transferred to a nitrocellulose membrane, and probed on with antibodies (blot), as indicated. Position of CAIV (filled arrow) and NBC1 (open arrow) are shown.

expression of these two proteins. HEK293 cells express low endogenous levels of CAII (Figure 4B, lane 1), and transfection with V143Y CAII increased the total CAII by approximately 20-fold (lanes 2 and 3).

*Immunoprecipitation of NBC1b/CAIV Complex.* NBC1a and CAIV are coexpressed in the basolateral membrane of the kidney proximal tubule. To examine whether they physically associate in the kidney, lysates of mouse kidney membranes were immunoprecipitatedwith anti-CAIV and anti-NBC1 antibodies. Immunoblots of kidney lysates revealed immunoreactive bands of 43 and 105 kDa, corresponding to CAIV (filled arrow) and NBC1 (open arrow), respectively (Figure 5). CAIV immunoprecipitated with anti-NBC1 antibody and NBC1 could be immunoprecipitated by the anti-CAIV antibody, thus indicating that CAIV and NBC1 interact in the kidney. Although these data show a specific interaction between CAIV and NBC1 in the kidney, some nonspecific bands were evident. The background reflects the difficulty of immunoprecipitation from the kidney where expression levels of NBC1 and CAIV are not high. As one indication of specificity of the immunopreciptations, we also immunoprecipitated using the irrelevant antibody, phospho-p44/42 MAP kinase, which like anti-CAIV, is a polyclonal antibody. When probed with an anti-NBC1 antibody, no immunoreactive material was detected at the molecular weight of NBC1b (Figure 5).

*GST Pull-Down Assays of NBC1/CAIV Interaction.* Since GPI-anchored CAIV faces the extracellular space, we reasoned that CAIV likely interacts with the extracellular region of NBC1, just as occurs with AE1 (*19*). A human NBC1b topology model (Figure 6A), developed on the basis of a human AE1 topology model (*30*), revealed EC3 and EC4 as the two strongest candidates for binding to extracellular-anchored CAIV because of their size.

GST fusion proteins of EC3 and EC4 (GST-NBC1EC3 and GST-NBC1EC4) were used in GST pull-down assays (Figure 6B). Blots were stripped and probed for GST, and the amount of CAIV associated with each protein per unit of GST was quantified. GST-NBC1EC4 bound 0.247 ± 0.004 CAIV/GST (lane 2), while levels were much lower for GST alone (0.030 ± 0.009) and GST-NBC1EC3 (0.097 ± 0.017) (lanes 1 and 3, respectively). Taken together, these results show that CAIV binds specifically to EC4 of human NBC1.

*Identification of the Amino Acid Sequence Required for NBC1/CAIV Interaction.* The alignment of putative EC4 regions of bicarbonate transport proteins shows four clusters of a conserved sequence, which are therefore candidate CAIV binding sites (Figure 7A). EC4 of rat AE1 bound CAIV (*19*), but EC4 of rat AE3 (GST-AE3EC4) did not bind CAIV, in a GST pull-down assay (Figure 7B, lane 2). Since NBC1EC4 and AE1EC4 (*19*) bind CAIV, while AE3EC4 does not (Figure 7B), NBC1 amino acids 766−768 could be involved in binding CAIV. Consistent with this possibility, NBC1 G767T mutation blocked the ability to bind CAIV in GST pull-down assays (Figure 7B, lane 4). The quantification of blots for bound CAIV and amount of applied GST protein confirmed that the G767T mutation blocked the interaction between NBC1 and CAIV (0.167 ± 0.02 CAIV/GST for GST-NBC1EC4 and 0.027 ± 0.005 for GST-NBC1G767T-EC4), while GST alone and GST-AE3EC3 bound little CAIV (0.013 ± 0.004 and 0.030 ± 0.008, respectively). Thus, CAIV likely interacts directly with the region surrounding G767T of NBC1.

The NBC1 G767T mutation did not affect the expression level (Figure 8A; NBC1 alone, 903 pixels; NBC1 G767T, 903 pixels; NBC1 G767T/V143Y CAII, 860 pixels; NBC1 G767T/V143Y CAII/CAIV, 903 pixels), or strikingly, the $pH_i$ recovery activity of NBC1 after imposed acid loads (3.05 ± 0.27 mM/min, $n = 5$), as compared to wild-type NBC1 (2.97 ± 0.31 mM/min) (Figure 8B). Coexpression of NBC1 G767T with CAIV failed to significantly increase the transport rate (3.29 ± 0.07 mM/min) (Figure 8B). V143Y CAII also impaired the transport activity of NBC1 G767T (Figures 2A and 8B). However, unlike wild-type NBC1 (Figures 1 and 2A), the loss of $pH_i$ recovery activity induced by V143Y CAII (2.30 ± 0.19 mM/min, $n = 5$) was not restored by CAIV coexpression (2.29 ± 0.16 mM/min, $n = 5$; Figure 8B). The fraction of NBC1 G767T processed to the cell surface was not significantly different whether it was expressed alone (27 ± 7%) or coexpressed with CAIV (30 ± 9%) (not shown). Taken together, these results are consistent with a failure of NBC1 G767T to interact with CAIV at the plasma membrane. We conclude that G767 is not directly involved in $HCO_3^-$ transport but forms an essential part of the CAIV binding site on the fourth extracellular loop of NBC1.

## DISCUSSION

Carbonic anhydrase enzymes and bicarbonate transport proteins are functionally coupled; carbonic anhydrases alternately produce or consume $HCO_3^-$, the substrate for bicarbonate transporters. Previously, the cytosolic enzyme, CAII, was found to interact with the plasma membrane $Cl^-/HCO_3^-$ exchangers AE1, AE2, and AE3 but not with the $Cl^-/HCO_3^-$ exchanger, DRA (*18*, *26*). Later, the extracellular-anchored enzyme, CAIV, was found to interact with AE1 (*19*). Here, we have shown interactions between CA enzymes and the $Na^+/HCO_3^-$ co-transporter, NBC1b. Physi-

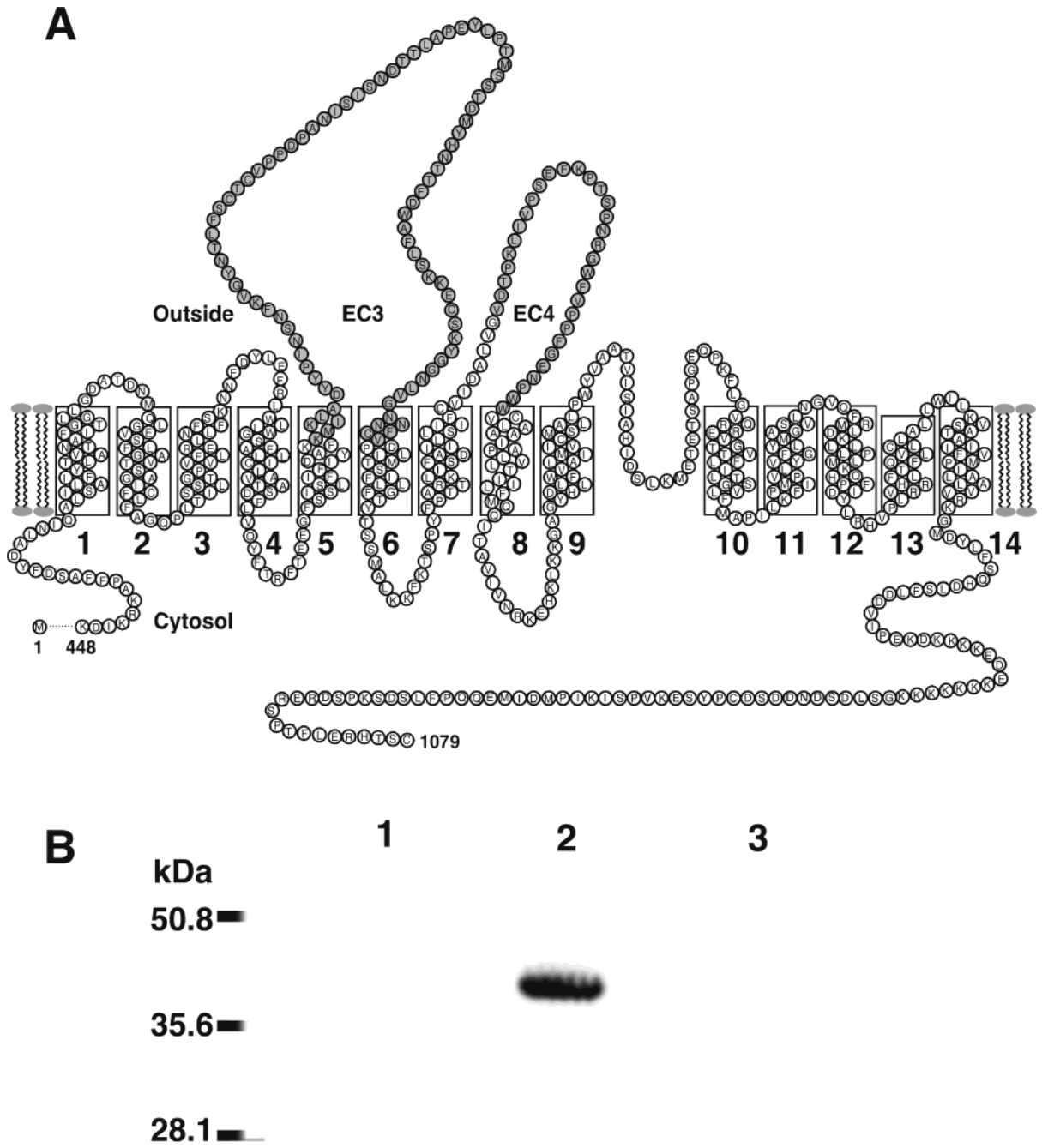


FIGURE 6: Topology model of human NBC1b and interaction of CAIV and NBC1. (A) Topology model of human NBC1b on the basis of the human AE1 topology model (*30*). Amino acids corresponding to GST-NBC1EC3 and EC4 are indicated in gray. (B) The proteins (250 $\mu$g) GST alone (lane 1), GST-NBC1EC4 (lane 2), and GST-NBC1EC3 (lane 3) were individually bound to glutathione sepharose resin. Lysates of HEK293 cells transfected with CAIV cDNA were applied to the resin and incubated overnight. Eluted proteins were resolved on 12% polyacrylamide gels, transferred to a PVDF membrane, and probed for CAIV.

cal interactions between NBC1b and CAIV were demonstrated by coimmunoprecipitations and GST pull-down assays, which indicated a specific interaction between CAIV and EC4 of NBC1. The inhibition of NBC1b $pH_i$ recovery activity by V143Y CAII suggests a dominant negative effect, which demonstrates a functional effect of CAII/NBC1b interaction. Modulation of the NBC1/CAII interaction has recently been postulated as a mode of NBC1 regulation (*31*). The expression of CAIV increased the activity of NBC1b. However, the G767T NBC1 mutant retained functional activity but did not functionally or physically interact with CAIV, which indicates that the region surrounding G767 forms the CAIV binding site. We conclude that CAIV and NBC1 interact at the plasma membrane and that this interaction is required for full NBC1 activity.

EC4 of NBC1 forms the binding site for CAIV. Although a binding site for CAIV would likely be formed from several amino acids, we found that the G767T NBC1 mutant did not interact with CAIV in GST pull-down assays. We conclude that amino acids 766−768 of human NBC1 are involved in binding to CAIV. However, it is possible that additional portions of the NBC1 extracellular surface are also involved in the CAIV interaction. A role of the large extracellular loops in NBC1 function, perhaps in substrate funneling to the transport site, was suggested by the result that antibodies against EC3 of NBC1 were able to inhibit

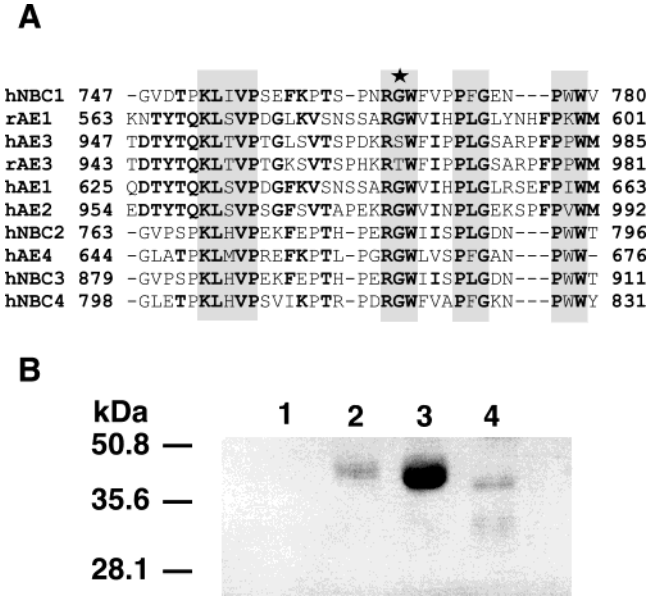


FIGURE 7: Alignment of amino acid sequences of bicarbonate transport proteins and identification of the amino acid sequence required for CAIV/NBC1 interaction. (A) Alignment of bicarbonate transporter extracellular loops. Sequence conservation is indicated by gray rectangles. Star indicates the position of the G767T mutation constructed in human NBC1. The first letter of each sequence name represents the species: h = human and r = rat. (B) Protein (250 $\mu$g/lane of GST alone (lane 1), GST-AE3EC4 (lane 2), GST-NBC1EC4 (lane 3), and GST-NBC1EC4-G767T mutant (lane 4)) was bound to glutathione sepharose resin. Lysates of HEK293 cells transfected with CAIV cDNA were applied to the resin and incubated overnight. Eluted proteins were resolved by SDS−PAGE on 12% polyacrylamide gels, transferred to PVDF membrane, and probed for CAIV.

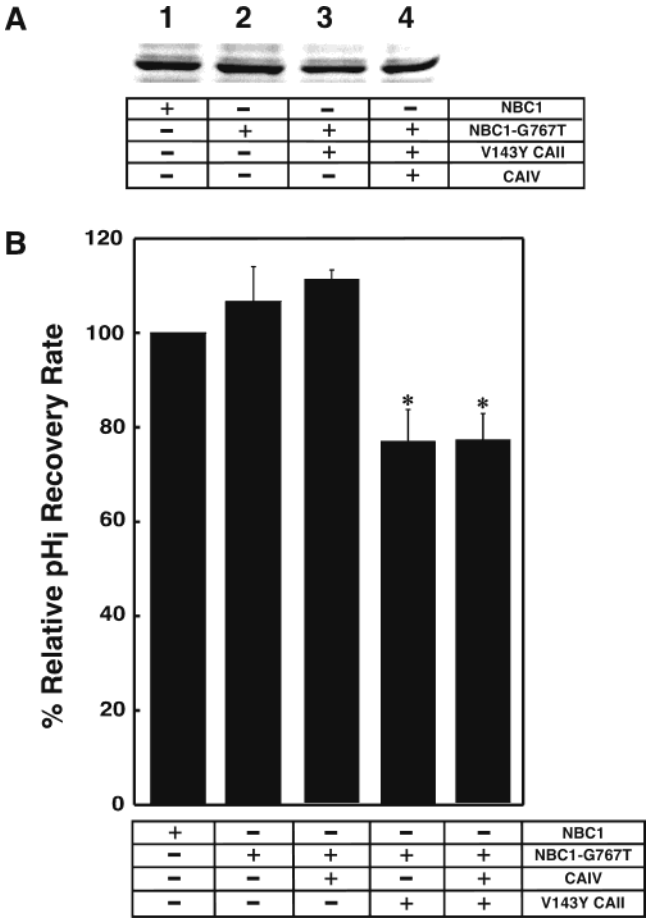


FIGURE 8: Expression and $pH_i$ recovery activity of the NBC1-G767T mutant. (A) HEK293 cells were transiently cotransfected with cDNA coding for NBC1, NBC1-G767T, CAII V143Y, and CAIV, as indicated in the figure. Two days post-transfection, cells were solubilized, and samples (5 $\mu$g of protein) were resolved by SDS−PAGE and transferred to PVDF membrane. Immunoblots were probed with rabbit polyclonal anti-rat NBC1 antibody. (B) Mean $pH_i$ recovery rates relative to NBC1. Asterisk represents statistical significance.

NBC1 activity (*11*). Since NBC1a and NBC1b have identical amino acid sequences in their entire membrane domain, their extracellular surfaces are identical, and the two proteins will interact identically with CAIV. We did not perform any experiments to identify the corresponding binding site on CAIV. However, inspection of the crystal structures for human CAII and CAIV reveals two structures that are very similar (*32*, *33*), but CAIV has a surface loop (G173−G179) that is not present in CAII. It is therefore tempting to speculate that this loop could form the NBC1 interaction site.

The present report confirms the one earlier observation that CAII interacts with NBC1 (*20*). Although we did not examine the mode of CAII/NBC1 interaction, the presence of CAII binding motifs in the NBC1 C-terminal region (*18*) suggests that NBC1 interacts with CAII in the same manner as does the AE1 $Cl^-/HCO_3^-$ exchanger. In this case, the acidic motif in the NBC1 C-terminus likely interacts with the exposed basic N-terminal region of CAII (*34*).

The presence of CAIV at the extracellular surface of NBC1 may accelerate the NBC1-mediated $pH_i$ recovery rate by the formation of a bicarbonate transport metabolon (*18*). A metabolon is a physical complex of proteins in a sequential metabolic pathway (*35*). We have found that $Cl^-/HCO_3^-$ exchangers associate to form a transport metabolon, a complex between a transporter and the enzyme that produces or consumes the transported substrate (*18*, *19*). This paper and one other have shown interactions between CAII and NBC1 to form the intracellular component of the transport metabolon (*20*).

The present study shows that CAIV is the extracellular component of the metabolon, which associates with NBC1 to facilitate $pH_i$ recovery activity. In HEK293 transfected with the AE1 $Cl^-/HCO_3^-$ exchanger, the total carbonic anhydrase activity has been estimated to be in excess of bicarbonate transport capacity (*18*). Since NBC1 has a lower turnover rate than AE1, if we assume similar levels of NBC1 expression to those for AE1, NBC1 is rate limiting to the combined action of CA catalysis and bicarbonate transport.

Increases of the NBC1 activity will therefore increase the coupled flux from carbonic anhydrase through the transporter. The rate of transport by NBC1 is proportional to the concentration gradient for $HCO_3^-$ across the membrane; transport is maximized by high local concentration of $HCO_3^-$ at the cis side of the membrane and low $HCO_3^-$ at the trans side. Binding of CAIV at EC4 localizes CAIV close to the extracellular NBC1 transport site. During cellular $HCO_3^-$ influx, for example, in the pancreas, the presence of CAIV localized to the NBC1 transport site will drive transport by increases of local $[HCO_3^-]$. Conversely, during cellular $HCO_3^-$ efflux, for example, in the renal proximal tubule, CAIV at the NBC1 transport site will optimize the rate of $HCO_3^-$ conversion to $CO_2$, thereby minimizing the $[HCO_3^-]$

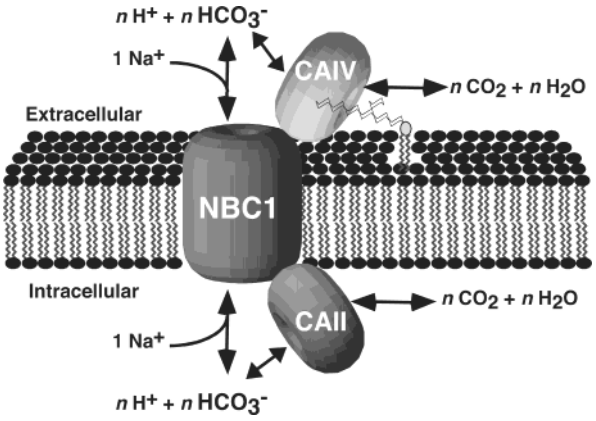


FIGURE 9: NBC1 bicarbonate transport indicating the push−pull effect of CAII and IV. Schematic model of the binding of extracellular CAIV and cytoplasmic CAII to NBC1 protein. The *n* beside the molecules in equilibrium denotes 2 or 3 since NBC1 is known to operate with a tissue-dependent $1Na^+:2-3HCO_3^-$ stoichiometry. The multi-molecular arrangement potentiates NBC-mediated bicarbonate flux by the production and removal of bicarbonate from the transport site. CAII and CAIV cooperate to push bicarbonate to the transport site and then pull from the opposite side of the membrane. The structure attached to the right-hand side of CAIV represents the GPI anchor that couples CAIV to the lipid bilayer.

at the external transport site, maximizing the transmembrane $[HCO_3^-]$ gradient local to NBC1, and maximizing the transport rate. The combined effects of CAII and CAIV provide a push−pull effect on transport (Figure 9). Another mechanism by which the CA/bicarbonate transporter interaction enhances $HCO_3^-$ flux is provided by the observation that the CAII catalytic rate increases when bound to peptides corresponding to the binding site of AE1 (*36*). Whether peptides corresponding to the NBC1b EC4 sequence activate CAIV awaits determination.

The functional assay we have used shows that CAIV interaction with NBC1 accelerates the rate of cellular $pH_i$ recovery. The simplest explanation for the observation is that interaction with CAIV accelerates the rate of bicarbonate transport by NBC1. Similarly, electrophysiological recordings recently showed that the interaction between CAII and NBC1 increased the NBC1 transport flux (*20*). All of the functional measurements relied on changes of $pH_i$ to report indirectly on the NBC1-mediated $HCO_3^-$ flux. It is therefore possible that the effects of CAIV/NBC1 interaction that we have observed reflect an effect on cytosolic $H^+$ handling within the cells rather than an effect on transport by NBC1. However, we consider this unlikely because functional assays in the presence and absence of the membrane-impermeant CAIV inhibitor showed that extracellular CAIV is required for the effects of CAIV on the recovery of $pH_i$.

Our results are significant to $HCO_3^-$ transport in tissues that coexpress CAIV and NBC1. The bulk of $HCO_3^-$ reabsorption in the kidney occurs in the proximal tubule. NBC1, which is present in the BLM of proximal tubules cells, is essential for $HCO_3^-$ reabsorption. NBC1 and CA interaction in the kidney has been postulated since the CA inhibitor, ACTZ, reduced the rate of $H^+$ secretion and $HCO_3^-$ reabsorption in the proximal tubule by at least 80% (*37*, *38*). Since ACTZ can inhibit NBC by decreasing the substrate availability for the NBC at the surface of BLM of kidney cells (*5*), it is likely that CAIV on the outer surface of BLM of proximal tubule stimulates $HCO_3^-$ reabsorption both directly via the NBC and indirectly by reducing $HCO_3^-$ concentrations in the area of $HCO_3^-$ efflux from NBC. Indeed, a membrane-impermeant CA inhibitor reduced proximal tubule $HCO_3^-$ reabsorption by 62% when applied only to the BLM surface (*13*). Similarly, contractile function of the heart is highly dependent on $pH_i$. In heart, inhibition of CA with ACTZ slowed the initial rate of change of $pH_i$ recovery after the acid load, suggesting that the efficiency of the NBC transport activity is dependent upon CA activity (*16*). Our results indicate that direct extracellular interaction of CAIV with NBC1 can maximize the $pH_i$ recovery after an acid load in cardiomyocytes.

The pancreas secretes $HCO_3^-$ at a concentration up to 145 mM (*39*). NBC1 is likely involved in the uptake of $HCO_3^-$ from the blood into pancreatic duct cells. Individuals homozygous for the ΔF508 allele of the CFTR gene develop cystic fibrosis and fail to secrete adequate levels of pancreatic $HCO_3^-$, which contributes to their pancreatic insufficiency. Wild-type CFTR, but not ΔF508 CFTR (the major cystic fibrosis allele), facilitates the appropriate membrane targeting of CAIV (*28*). Combining this result with the findings in the present paper, we propose that in pancreatic duct cells cellular $HCO_3^-$ loading requires NBC1 activity. In turn, full NBC1 activity requires interaction between CAIV and NBC1. The failure of ΔF508 CFTR to bring CAIV to the plasma membrane would effectively reduce NBC1 activity, as seen in our experiments, thereby reducing pancreatic $HCO_3^-$ secretion.

We have presented evidence that there are physical and functional interactions between extracellular CAIV and the human NBC1b $Na^+/HCO_3^-$ co-transporter. Amino acids 766−768 of NBC1 were identified as required for the CAIV/NBC1 interaction. Direct interaction between CAIV and NBC1 is needed for maximal rate of recovery of $pH_i$ by NBC1. Together, CAIV and human NBC1 form the extracellular component of a bicarbonate transport metabolon, the complex of cytosolic CAII, transmembrane NBC1, and extracellular CAIV, which maximizes the transmembrane $HCO_3^-$ flux. Maximization of NBC1 transport activity by interaction with CAIV may provide a better explanation for physiological roles of these two proteins in mammalian tissues.

## ACKNOWLEDGMENT

We thank Dr. Antoine Bril (GlaxoSmithKline, Philadelphia, PA) for NBC1b cDNA and Dr. Manoocher Soleimani for affinity purified anti-NBC1 antibody.

## REFERENCES

1. Boron, W. F., and Boulpaep, E. L. (1989) *Kidney Int. 36*, 392−402.
2. Soleimani, M., and Burnham, C. E. (2001) *J. Membr. Biol. 183*, 71−84.
3. Burnham, C. E., Amlal, H., Wang, Z., Shull, G. E., and Soleimani, M. (1997) *J. Biol. Chem. 272*, 19111−4.
4. Alpern, R. J. (1985) *J. Gen. Physiol. 86*, 613−36.
5. Soleimani, M., Grassi, S. M., and Aronson, P. S. (1987) *J. Clin. Invest. 79*, 1276−80.
6. Alpern, R. J. (1990) *Physiol. Rev. 70*, 79−114.
7. Soleimani, M., and Singh, G. (1995) *J. Invest. Med. 43*, 419−30.
8. Abuladze, N., Lee, I., Newman, D., Hwang, J., Boorer, K., Pushkin, A., and Kurtz, I. (1998) *J. Biol. Chem. 273*, 17689−95.

9. Choi, I., Romero, M. F., Khandoudi, N., Bril, A., and Boron, W. F. (1999) *Am. J. Physiol. 276*, C576−584.
10. Gross, E., Abuladze, N., Pushkin, A., Kurtz, I., and Cotton, C. U. (2001) *J. Physiol. 531*, 375−82.
11. Khandoudi, N., Albadine, J., Robert, P., Krief, S., Berrebi-Bertrand, I., Martin, X., Bevensee, M. O., Boron, W. F., and Bril, A. (2001) *Cardiovasc. Res. 52*, 387−96.
12. Schwartz, G. J. (2002) *J. Nephrol. 15*, S61−74.
13. Tsuruoka, S., Swenson, E. R., Petrovic, S., Fujimura, A., and Schwartz, G. J. (2001) *Am. J. Physiol.: Renal, Fluid Electrolyte Physiol. 280*, F146−54.
14. Fujikawa-Adachi, K., Nishimori, I., Sakamoto, S., Morita, M., Onishi, S., Yonezawa, S., and Hollingsworth, M. A. (1999) *Pancreas 18*, 329−35.
15. Sender, S., Decker, B., Fenske, C. D., Sly, W. S., Carter, N. D., and Gros, G. (1998) *J. Histochem. Cytochem. 46*, 855−61.
16. Lagadic-Gossmann, D., Buckler, K. J., and Vaughan-Jones, R. D. (1992) *J. Physiol. 458*, 361−84.
17. Vince, J. W., and Reithmeier, R. A. F. (1998) *J. Biol. Chem. 273*, 28430−7.
18. Sterling, D., Reithmeier, R. A., and Casey, J. R. (2001) *J. Biol. Chem. 276*, 47886−94.
19. Sterling, D., Alvarez, B. V., and Casey, J. R. (2002) *J. Biol. Chem. 277*, 25239−46.
20. Gross, E., Pushkin, A., Abuladze, N., Fedotoff, O., and Kurtz, I. (2002) *J. Physiol. 544*, 679−85.
21. Schwartz, G. J., Kittelberger, A. M., Barnhart, D. A., and Vijayakumar, S. (2000) *Am. J. Physiol.: Renal, Fluid Electrolyte Physiol. 278*, F894−904.
22. Sarkar, G., and Sommer, S. S. (1990) *Biotechniques 8*, 404−7.
23. Ruetz, S., Lindsey, A. E., Ward, C. L., and Kopito, R. R. (1993) *J. Cell. Biol. 121*, 37−48.
24. Laemmli, U. K. (1970) *Nature 227*, 680−5.
25. Thomas, J. A., Buchsbaum, R. N., Zimniak, A., and Racker, E. (1979) *Biochemistry 18*, 2210−2218.
26. Sterling, D., Brown, N. J., Supuran, C. T., and Casey, J. R. (2002) *Am. J. Physiol.: Cell. Physiol. 283*, C1522−9.
27. Scozzafava, A., Briganti, F., Ilies, M. A., and Supuran, C. T. (2000) *J. Med. Chem. 43*, 292−300.
28. Fanjul, M., Salvador, C., Alvarez, L., Cantet, S., and Hollande, E. (2002) *Eur. J. Cell. Biol. 81*, 437−47.
29. Fujinaga, J., Loiselle, F. B., and Casey, J. R. (2003) *Biochem. J. 371*, 687−96.
30. Tang, X. B., Fujinaga, J., Kopito, R., and Casey, J. R. (1998) *J. Biol. Chem. 273*, 22545−53.
31. Gross, E., and Kurtz, I. (2002) *Am. J. Physiol.: Renal, Fluid Electrolyte Physiol. 283*, F876−87.
32. Stams, T., Nair, S. K., Okuyama, T., Waheed, A., Sly, W. S., and Christianson, D. W. (1996) *Proc. Natl. Acad. Sci. U.S.A. 93*, 13589−94.
33. Lesburg, C. A., Huang, C., Christianson, D. W., and Fierke, C. A. (1997) *Biochemistry 36*, 15780−91.
34. Vince, J. W., Carlsson, U., and Reithmeier, R. A. (2000) *Biochemistry 39*, 13344−9.
35. Srere, P. A. (1985) *Trends Biochem. Sci. 10*, 109−10.
36. Scozzafava, A., and Supuran, C. T. (2002) *Bioorg. Med. Chem. Lett. 12*, 1177−80.
37. Cogan, M. G., Maddox, D. A., Warnock, D. G., Lin, E. T., and Rector, F. C., Jr. (1979) *Am. J. Physiol. 237*, F447−54.
38. Lucci, M. S., Warnock, D. G., and Rector, F. C., Jr. (1979) *Am. J. Physiol. 236*, F58−65.
39. Guyton, A. C. (1987) *Human Physiology and Mechanisms of Disease*, 4th ed., W. B. Saunders, Philadelphia.

BI0353124